Desalination and Water Treatment
www.deswater.com

doi: 10.5004/dwt.2023.29235

286 (2023) 136–149
February

Efficient catalytic ozonation over CuO/ZnO for ofloxacin degradation: the synergistic effect between CuO and ZnO promotes the catalytic effect

Zicai Zhao[a,c], Yuanyuan Zhang[a,b,*], Shuangfei Wang[a], Hongxiang Zhu[a], Jianhua Xiong[a,c]

[a]*Guangxi Key Laboratory of Clean Pulp and Papermaking and Pollution Control, College of Light Industry and Food Engineering, Guangxi University, Nanning 530004, emails: jiedeng05@sina.com (Y. Zhang), 1027143182@qq.com (Z. Zhao), 545155727@qq.com (S. Wang), 550104626@qq.com (H. Zhu), 2653841837@qq.com (J. Xiong)*
[b]*School of Marine Sciences, Guangxi University, Nanning 530004*
[c]*School of Resources, Environment and Materials, Guangxi University, Nanning 530004, China*

Received 12 August 2022; Accepted 16 December 2022

ABSTRACT

In this study, zinc oxide (ZnO) supported copper oxide (CuO) catalyst was prepared and characterized. Ofloxacin (OFL) was selected as the target pollutant to study the catalytic activity of CuO/ZnO. The characterizations of CuO/ZnO were studied using X-ray diffraction, field emission scanning electron microscopy and X-ray photoelectron spectroscopy etc. The catalytic activity of CuO/ZnO on OFL degradation efficiency was systematically examined under different experimental conditions: including different catalyst doses, O_3 flow rates, initial pH values and OFL concentrations. The catalytic activity achieved maximal when Cu:Zn was 1:5. The results showed that the degradation of OFL increased with the increase of CuO/ZnO dosage, O_3 flow rate and pH value, but decreased with the increase of OFL initial concentration. Under selected initial conditions (80 mL/min ozone flow, 20 mg/L OFL solution, and 0.63 g/L catalyst dosage), the O^3+CuO/ZnO process significantly improved OFL removal efficiency due to the production of hydroxyl radical (•OH), which was approved by tert-butanol (TBA). It was confirmed that CuO and ZnO showed synergistic effect on the catalytic ozonation of OFL. The degradation efficiency of OFL was only slightly decreased after five repeated times, indicating that CuO/ZnO had well catalytic stability.

Keywords: Zinc oxide; Copper oxide; Ofloxacin; Catalytic ozonation; Catalytic activity

1. Introduction

In recent years, the increasing applications of antibiotics adversely affect the water environment due to their stability and biological resistance [1]. For example, ciprofloxacin (CPF), amoxicillin, ofloxacin (OFL) and norfloxacin (NOR) have been frequently detected at concentrations ranging from ng/L to mg/L levels in domestic and hospital effluents [2,3]. The effluents of pharmaceutical manufacturing facilities show higher levels with even up to mg/L [4]. As a typical fluoroquinolone antibiotic, ofloxacin (OFL) has been widely used and accumulated in the water bodies [5]. OFL can hardly be degraded by the conventional water treatment processes and cause serious risk to the environment [6,7]. Therefore, it is very important to develop effective, practical and economical methods to degrade these organic pollutants in water [8,9]. At present, effective treatment methods of antibiotics were biological treatment, physical adsorption and advanced oxidation [10–12].

Advanced oxidation processes (AOPs) can oxidize resistant organic pollutants to CO_2 and H_2O due to the

* Corresponding author.

generation of active free radicals [13]. The current advanced oxidation technologies include photocatalytic oxidation, Fenton reagent, ozone oxidation and activated persulfate [14]. Among the AOPs, heterogeneous catalytic ozonation is a proven powerful technology and has been successfully used for degrading antibiotics in the past few years [13]. Solid catalysts with high efficiency and stability have widely been studied. These catalysts which comprise metal oxides, carbon-based materials and metal/metal oxides on supporters generate reactive hydroxyl radicals (•OH) by interacting with ozone (O_3) [15].

Zinc oxide (ZnO) have been studied in the fields of photocatalytic and catalytic ozonation as a result of their superiorities of high catalytic ability, low cost and low toxicity [16]. For example, Jung et al. [17] found that nanosized ZnO significantly enhanced the degradation of *p*CBA in catalytic ozone system. Taie et al. [18] reported that UV/ZnO and O_3/ZnO processes could significantly enhance the removal rate of trimethoprim (TMP) using zinc oxide as catalyst. It was reported that doping metal into metal oxide could enhance the interfacial electron transfer of composite metal oxides, thus increasing the activity of the catalyst [19,20]. Shen et al. [21] reported that magnesium-doped ZnO was used as a catalysts for ozonation. The removal efficiency of TOC was 50% higher than that of ozone alone.

Copper oxide (CuO) was another proverbial *p*-type semiconductor with low toxicity and high stability. In recent years, CuO has been vastly investigated in various areas [22,23]. For instance, Turkay et al. [24] studied the degradation of humic acid (HA) in the CuO catalytic ozonation system. The results revealed that the degradation of HA by catalytic ozonation existence of CuO was found to be much more valid than the ozonation process alone, and the degradation efficiency of HA CuO reached 87% in 5 min. Liu et al. [25]reported that different amounts of CuO modified graphitic carbon nitride (g-C_3N_4) were successfully prepared and applied for catalyzed ozonation of oxalic acid (OA). The results indicated that when the mass ratio of CuO/g-C_3N_4 was 10, the OA removal efficiency reached 97.9% after 30 min at pH 5.0 [25].

The combination of ZnO and CuO in photocatalysis has been reported. For example, Samad et al. [26] investigated the photocatalytic oxidation of arsenite by CuO/ZnO under UV irradiation. The results showed that CuO has a significant effect on the photocatalytic performance of ZnO. Meanwhile, the rate constant of photocatalytic oxidation with CuO/ZnO was 4 times better than those obtained with pristine ZnO [15,26]. However, there are few studies on O_3 catalysis by ZnO/CuO. Considering the potential synergistic catalytic effects of ZnO and CuO, it was expected that the binary catalyst of CuO mixing with ZnO could show a better catalytic effect than the unitary catalyst [26–28]. In this work, CuO/ZnO composites were fabricated by wet impregnation method and selected OFL as the target contaminant. The major works were completed in the following aspects: (1) to characterize ZnO, CuO and CuO/ZnO composites; (2) to discuss the catalyst activities under different experimental conditions (e.g., catalyst dosage, solution pH, contaminant concentration and oxygen flow of ozone generator); (3) verify the stability of CuO/ZnO composite catalyst for ozone oxidation.

2. Experimental set-up

2.1. Materials and chemicals

OFL was purchased from Meilun Biological Technology Co., Ltd., (Dalian, China), zinc nitrate hexahydrate ($Zn(NO_3)_2{\cdot}6H_2O$) and cupric nitrate ($Cu(NO_3)_2{\cdot}3H_2O$) were bought from Kelong Chemicals Co., Ltd., (Chengdu, China). HCl (hydrochloric acid, 36%) was purchased from Lingfeng Chemical Reagent (Shanghai, China). NaOH (sodium hydroxide) was purchased from Aladdin Biochemical Technology Co., Ltd., (Shanghai, China). TBA (tert-butanol) was purchased from Damao Chemical Reagent Factory (Tianjin, China). BA (benzoic acid) was purchased from Maclean Biochemical Technology Co., Ltd., (Shanghai, China). All the above chemical reagents were analytical grade and used without further purification. Ultra-pure water which was used as the experimental water was obtained from Millipore Mili-Q Ultrapure Gradient A10 purification system.

2.2. Preparation of catalyst

CuO/ZnO was prepared by impregnating ZnO (prepared by calcination of $Zn(NO_3)_2{\cdot}6H_2O$ at 550°C for 5 h in air) with a water solution including a certain amount of $Cu(NO_3)_2{\cdot}3H_2O$ for 24 h. The sample was dried and the water was evaporated and then calcined at 300°C in the air for 1 h. The initial mass ratio of Cu:Zn = 1:5.

2.3. Characterization of catalyst

The crystal phase of samples was identified by X-ray diffraction (XRD) analysis (Rigaku Ultima IV, Japan; Cu Kα radiation, λ = 1.54,178 Å) in the 2θ range of 20°–80°. The morphology of samples was observed by field-emission scanning electron microscope (FESEM) equipped with an energy dispersive X-ray spectrometer (EDS) for elemental mapping. The samples were further verified by High-resolution JEM1200 transmission electron microscope (HRTEM, JEOL, Japan). The lattice spacing *d* was computed by TEM-Gatan digital Micrography. The chemical composition and state of element were confirmed by an X-ray photoelectron spectroscopy (XPS) spectrum (Thermo Scientific ESCALAB 250Xi). The Brunauer–Emmett–Teller (BET) surface area, HK pore size distribution and BJH pore size of the composites was estimated on the nitrogen adsorption–desorption isotherm. An inductively coupled plasma optical emission spectrometry (ICP-OES, optima 5300DV, PerkinElmer) was used to determine the leaching concentration of copper in the solution.

2.4. Catalytic tests

The catalytic ozone activities of catalyst were estimated by the degradation of OFL. Ozonation experiments were proceeded in a quartz tube of 100 mL. Before experiment of catalytic ozonation, the solution pH was adjusted by dedicated HCl and NaOH solution and 50 mg catalyst was added to OFL (80 mL, 20 mg/L) solutions. The mixture was constantly stirred with a magnetic stirrer. In the degradation processes, the O_3 generator was continuously generated and imported O_3 to the quartz tube and produced a series of reactions with the mixture. The ozone flow rate was 80 mL/

min. At fixed interval, 3.0 mL samples were collected from quartz tube and passed through a 0.45 um Millipore filter for further analysis. The concentration of OFL was measured using ultraviolet spectrophotometry.

3. Results and discussion

3.1. Physical properties of catalystsThe crystal phases of ZnO, CuO and CuO/ZnO were first scanned by XRD. As presented in Fig. 1a, ZnO can be indexed to hexagonal crystal ZnO with typical characteristic peaks at 2θ = 31.91°, 34.6°, 36.4°, 47.7°, 56.7°, 63.0°, 66.4°, 68.1°, and 69.2° (PDF 99-0111), corresponding to the crystal planes of (1 0 0), (0 0 2), (1 0 1), (1 0 2), (1 1 0), (1 0 3), (2 0 0), (1 1 2) and (2 0 1), respectively [29]. CuO revealed monoclinic structure (PDF 801916) with characteristic peaks at 2θ = 32.5°, 35.5° and 38.7°, corresponding to the crystal planes of (1 1 0), (–1 1 1) and (1 1 1), respectively [30]. In addition, the characteristic peak of CuO/ZnO was locally magnified. As shown in Fig. 1b, the diffraction peaks of mono clinic CuO and hexagonal ZnO can be obviously observed in the CuO/ZnO, proving that CuO was successfully mixed with ZnO.

The morphologies and structures of the catalysts were characterized by FESEM, HRTEM and relevant EDS elemental mapping analysis. It can be seen from Fig. 2a that ZnO was nanorods with different sizes. As illustrated in Fig. 2b, pure CuO was irregular flaky intermixed with small strip. As shown in Fig. 2c, the morphology of ZnO changed significantly after CuO was added. CuO/ZnO presented irregular aggregation in the surface. Meanwhile, the EDS-mapping

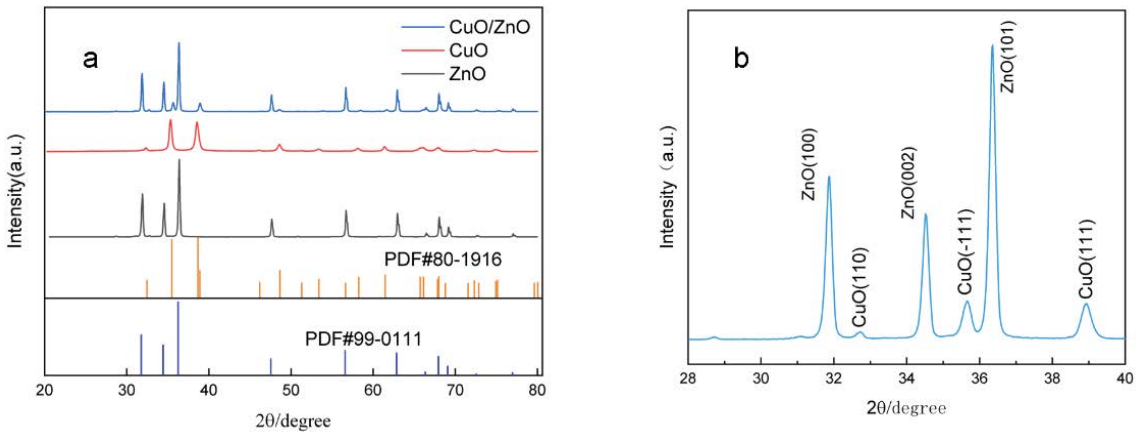

Fig. 1. (a) XRD spectra of different catalysts and (b) locally zoomed XRD spectra of CuO/ZnO.

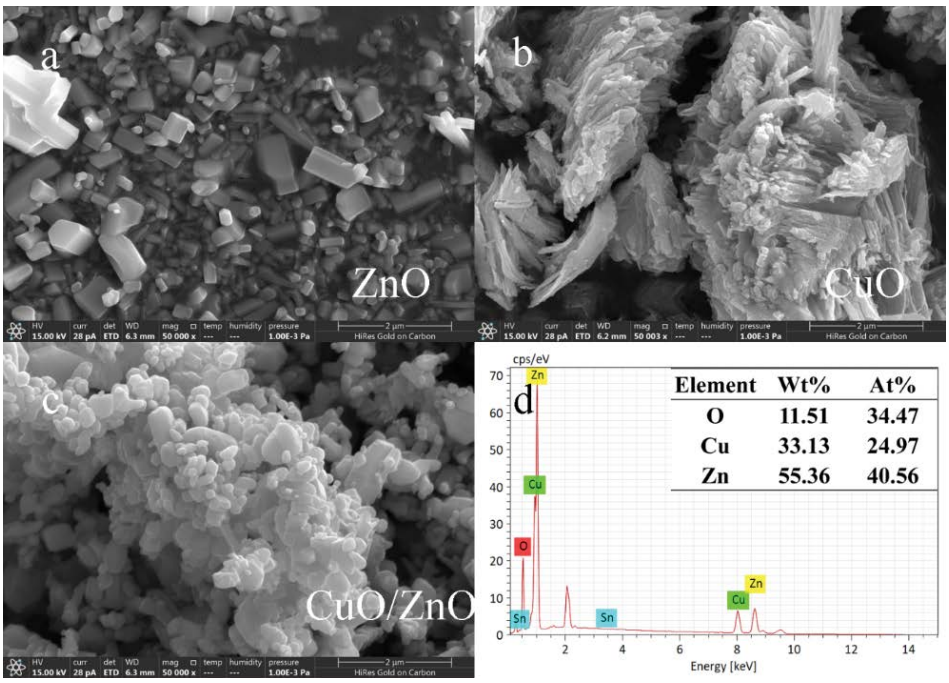

Fig. 2. FESEM images and EDS mapping of catalysts. (a) ZnO, (b) CuO, (c) CuO/ZnO, and (d) EDS results.

scan of CuO/ZnO was carried out to analyze the elemental constituents and distribution. According to the EDS consequences (Fig. 2d), a relatively well distribution of Zn, Cu and O over CuO/ZnO was clearly detected. The content of Zn, Cu and O was 55.36, 33.13 and 11.51 wt.% for CuO/ZnO, respectively. The detailed information of crystal plane and lattice spacing were further characterized by HRTEM. As shown in Fig. 3a, ZnO particles presented nanorod appearance with the size of ca.100–200 nm. The lattice spacing was 0.246 nm corresponding to the (101) plane of ZnO (Fig. 3b) [32]. Fig. 3c revealed that CuO was made up of irregular nanosheet structure [32]. The lattice spacing was 0.236 nm corresponding to the (1 1 1) plane of CuO (Fig. 3d) [33]. As shown in Fig. 3e, the boundary of CuO/ZnO was obscured, which may be attributed to that doping of CuO restrained the crystallization of ZnO and facilitated surface particle agglomeration. The image presented the lattice spacing of 0.246 and 0.236 nm in CuO/ZnO (Fig. 3f) indicating CuO was loaded on ZnO instead of entering the lattice, without destroying the lattice characteristics. The particle size distribution of CuO-ZnO catalyst was shown in Fig. 3g, the average particle size was about 0.3 um.

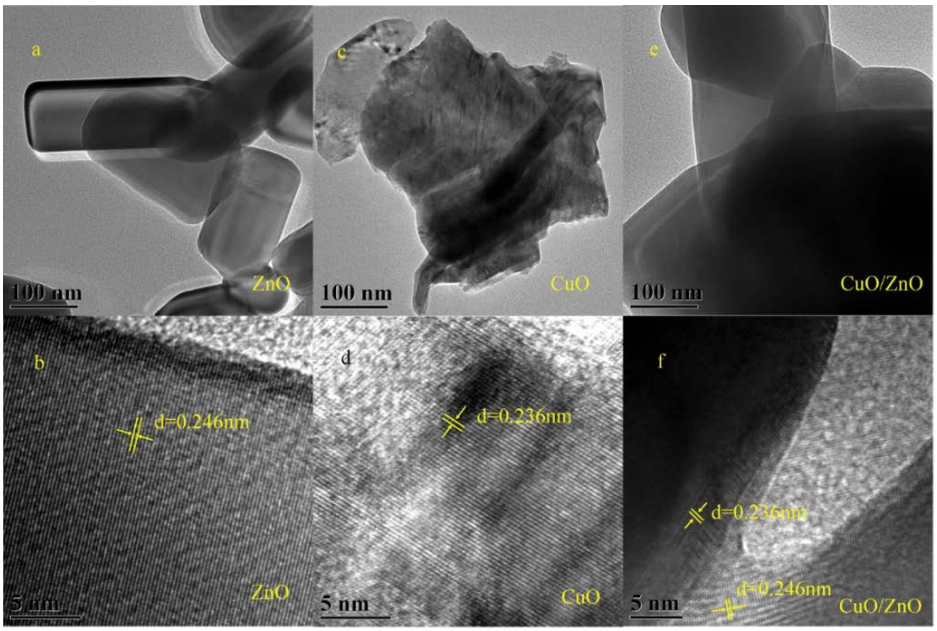

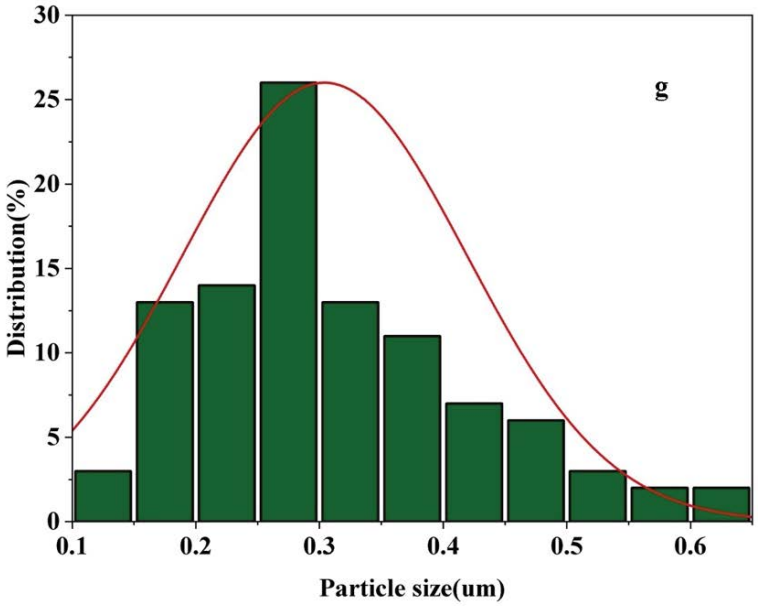

Fig. 3. (a,c,e) HRTEM images of catalysts, (b,d,f) lattice fringe spacing images of catalysts, and (g) particle size distribution of CuO/ZnO.

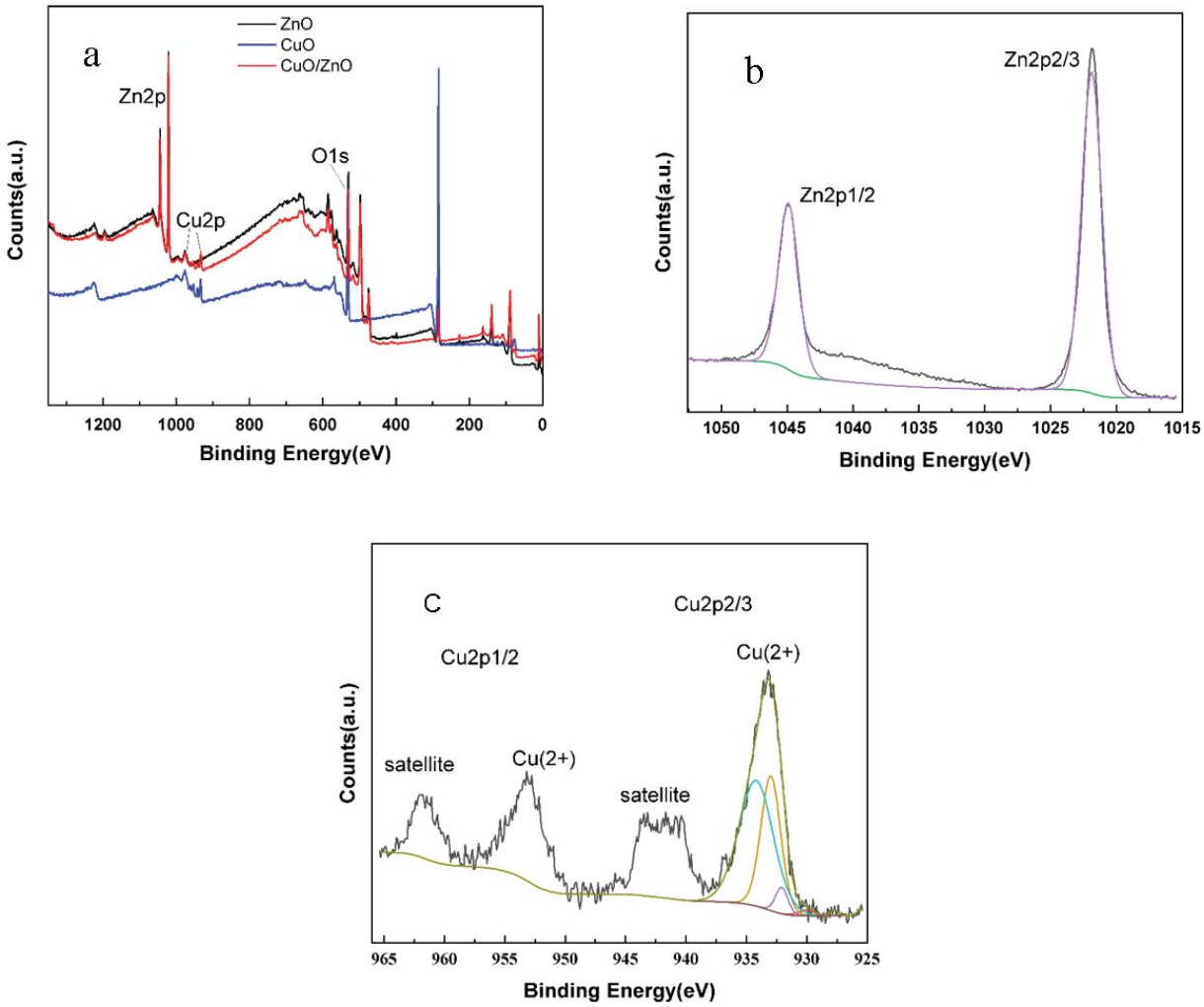

Fig. 4. XPS spectra of different catalyst. (a) XPS survey spectra of the catalysts, (b) Zn 2p of CuO /ZnO, and (c) Cu 2p of CuO/ZnO.

The chemical state and composition of ZnO, CuO and CuO/ZnO were further carefully verified by XPS (Fig. 4a). The Zn 2p, Cu 2p and O1s peaks were observed clearly in XPS survey spectrums of CuO/ZnO. As shown in Fig. 4b, the two peaks at 1,021.9 and 1,045.0 eV of Zn 2p spectra could be attributed to Zn 2p3/2 and Zn 2p1/2, respectively. The spin orbit split of 23 eV indicated the presence of ≡ZnII in CuO/ZnO [34]. As shown in Fig. 4c, the peaks located at 954.17 eV(Cu 2p1/2) and 934.17 eV (Cu 2p3/2) with a doublet separation of 20 eV, as well as the two strong satellites at 962.78 and 941.68 eV verified the presence of ≡CuII in CuO/ZnO [35,36].

Fig. 5 gives the nitrogen adsorption isotherms of ZnO and CuO/ZnO. The isotherms showed typical type IV patterns indicating that the two catalysts involved mesopores [37]. According to Table 1, although the pore size of CuO/ZnO was larger than that of ZnO, the pore volume and specific surface area reduced. The specific surface area and pore volume reduced from 6.413 to 3.317 m^2/g and 1.345 to 1.123 cm^3/g with CuO doping, respectively, which may be due to the surface covering and pore filling of the CuO [38]. In addition, the specific surface areas of both ZnO and CuO/ZnO were relatively small, indicating that the degradation of organic compounds may be attributed to the free radicals produced by O_3 catalysis rather than adsorption.

3.2. Catalytic activities of catalysts

The activities of catalysts on O_3 catalysis were evaluated through the degradation of OFL in different processes. As shown in Fig. 6a, the OFL degradation efficiency by O_3, O_3+ZnO, O_3+CuO after 30 min was 74%, 76% and 78%, respectively. By comparison, the degradation efficiency obviously increased to 88% in O_3+CuO/ZnO system. The degradation effect of CuO/ZnO as a catalyst of O_3 was distinct indicating that there might be synergies between CuO and ZnO. In order to show the advantages of the experimental results, the experimental results of this paper were compared with other literatures, and the results are shown in Table S1. Compared with the research results of Lu et al. [39] and Scaratti et al. [40], the degradation rate of pollutants in this paper was higher and the effect was better. Compared with the research results of Huang et al. and Abdedayem et al. [41,42], the ozone flow rate and catalyst dosage in this

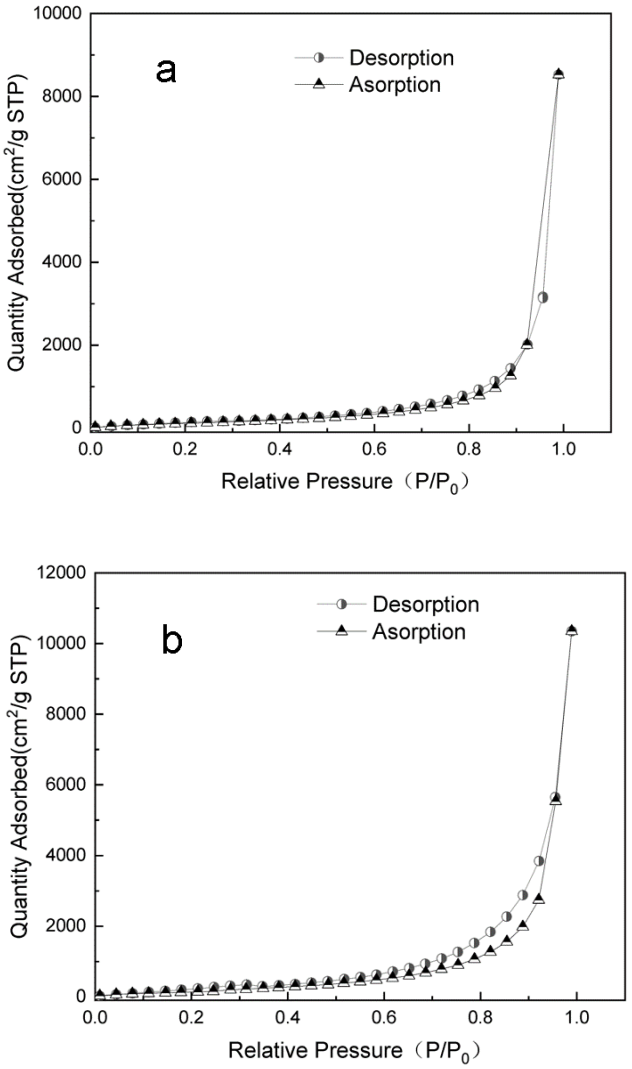

Fig. 5. N_2 adsorption/desorption isotherms of catalysts (a) ZnO and (b) CuO/ZnO.

paper were lower than the previous two, which has a low cost. Moreover, compared with the research results of Tang et al. [43], the ozone flow rate and catalyst dosage in this paper were smaller than the former.

3.3. Effect of Cu loading content on catalytic ozonation of OFL

Moreover, the metal loading on the catalyst surface has a great influence on the redox properties and catalytic activity of the catalyst. Therefore, OFL degradation in catalytic ozonation systems under CuO/ZnO catalyst with different mass ratio of Cu to Zn was studied. As shown in Fig. 6b, When the mass ratio of Cu to Zn increased from 1:10 to 1:5, the degradation efficiency of OFL increased from 40% to 57% after reaction of 10 min. However, with increasing mass ratio of Cu to Zn from 1:5 to 1:3 and 1:2.5, the degradation efficiency of OFL decreased to 30% and 25%, respectively. The phenomenon was consistent with those reported in the literature. For example, Huang et al. [41] investigated the catalytic activity of Fe/SBA-15 for ozonation of dimethyl phthalate in aqueous solution and discussed the removal effect of Fe/SBA-15 with different load ratios on dimethyl phthalate. The results showed that when the load ratio increased from 0% to 0.5%, the removal rate increased from 71.6% to nearly 100% in 30 min. However, when the load ratio increased to 2.0% and 4.0%, the degradation rate decreased to 95% and 76.2%. The reason may be attributed to the surface active sites of CuO/ZnO increased with the increase of CuO content, but overload of CuO may enhance the steric

Table 1
BET surface areas, pore volumes, and mean pore diameters of ZnO and CuO/ZnO.

Catalysts	Surface area (m^2/g)	Pore volume (cm^3/g)	Pore diameter (Å)
ZnO	6.413	0.01345	41.9363
CuO/ZnO	3.307	0.01123	67.9

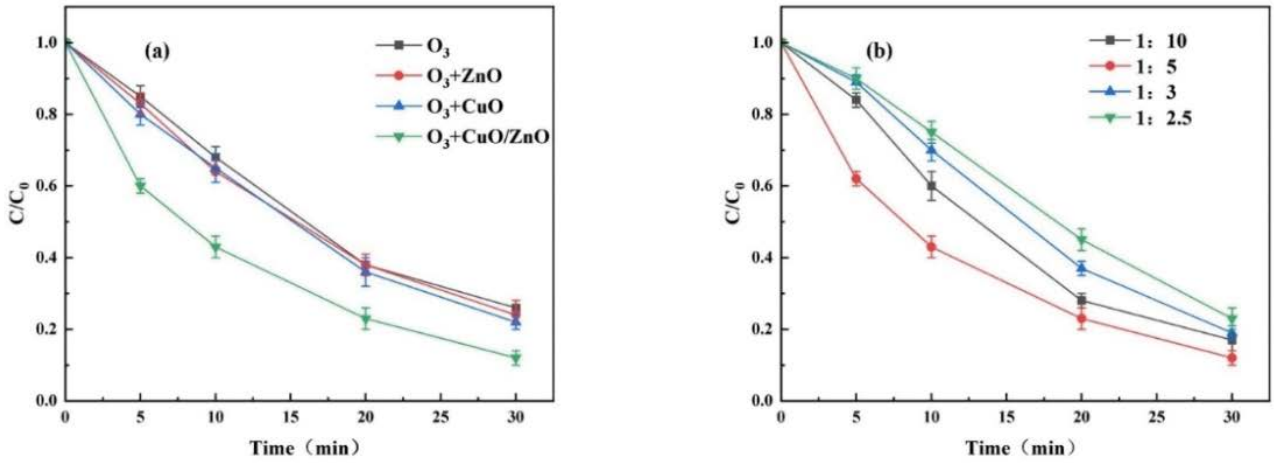

Fig. 6. Degradation of OFL in different catalytic ozonation systems (a) different catalysts. (b) CuO/ZnO with different mass ratio of Cu:Zn (Experimental conditions: $[OFL]_0$ = 20 mg/L, [ZnO] = [CuO] = [CuO/ZnO] = 0.63 g/L, $[O_3]$ = 80 mL/min, pH = 6.0).

hindrance of the catalyst and reduce the specific surface area of the catalyst [44]. Therefore, the optimum mass ratio of Cu to Zn in the catalytic ozonation OFL process was 1:5 and the catalyst was chosen for the following studies.

3.4. Synergistic effect for processes

The high efficiency of O_3+CuO/ZnO catalytic ozonation process indicated that the synergistic effect between the components can produce more active free radicals [45]. Through the pseudo-first-order rate constant and second-order kinetic constant of the O_3+CuO/ZnO reaction, the synergistic exponent (SI) can be obtained by calculating the following Eq. (1):

$$SI = \frac{k_{CuO/ZnO}}{k_{CuO} + k_{ZnO}} \quad (1)$$

The reaction kinetics of different processes to OFL and the reaction rate constants were shown in Fig. S1 and Table S2. The calculated SI value was 1.25 > 1, indicating that there was a synergistic effect between CuO and ZnO components.

3.5. Effect of catalyst dosage

To study the effects of different parameters on the degradation of OFL, batch experiments were performed under different conditions. The catalyst dosage was one of the important parameters in the catalytic ozonation system. As shown in Fig. 7a, the degradation rate of OFL was greatly improved with increasing the dosage of the CuO/ZnO from 0.31 to 1.24 g/L. The degradation rate of OFL in catalytic ozonation system after 30 min was 63.3%, 88%, 89% and 97%, respectively. The main reason for the result may be that the more catalysts, the more active sites and the more •OH induced which improves the oxidation efficiency of OFL [46]. Moreover, more dosage of catalyst could improve the utilization efficiency of O_3. Therefore, the degradation of OFL has a very important relationship with the dosage of catalyst [47]. After further increasing the dosage of catalyst

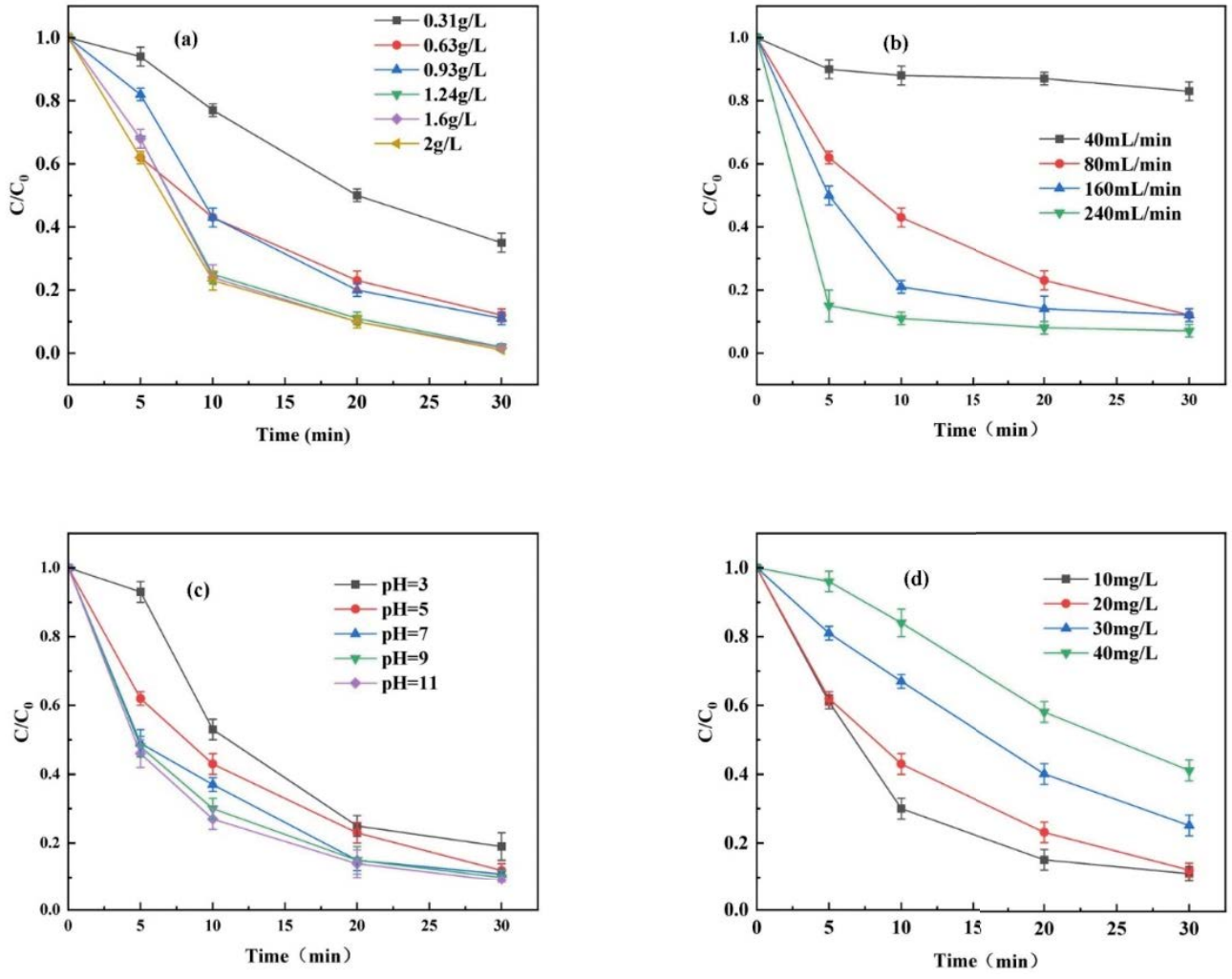

Fig. 7. Effect of various parameters on degradation of OFL. (a) catalyst dosage, (b) O_3 flow rate, (c) pH value, and (d) initial OFL concentration. Parameter values other than variables: [CuO/ZnO] = 0.63 g/L, $[OFL]_0$ = 20 mg/L, $[O_3]$ = 80 mL/min, pH = 6.0.

to 1.6 or 2 g/L, it was found that the catalytic effect was not greatly improved. Currently, 1.24 g/L catalyst dosage is the best dosage.

3.6. Effect of ozone concentration

As the oxidant, O_3 concentration was an important parameter for the catalytic ozonation system. The experiments were conducted with the aqueous O_3 flow rate of 40, 80,160 and 240 mL/min, respectively. As shown in Fig. 7b, the degradation of OFL increased quickly with O_3 flow rate increased from 40 to 160 mL/min. After reaction of 30 min, the degradation efficiency of OFL was only 20% at O_3 flow rate of 40 mL/min and the degradation efficiency was more than 80% at O_3 flow rate of 160 mL/min only after 10 min reaction. However, the degradation of OFL decreased when the O_3 flow rate was increased from 160 to 240 mL/min [48]. The reasons may be attributed to the finite active sites on CuO/ZnO surface, which would restrain the transfer rate of O_3 from the aqueous phase to the catalyst surface. On the other hand, excessive O_3 was a scavenger of •OH and inhibited the reaction between •OH and OFL [49].

3.7. Effect of pH solution

The pH value of the solution has a great effect on the decomposition of O_3 and the formation of active radicals as well as surface properties of catalyst [50,51]. As shown in Fig. 7c, the degradation of OFL was studied by varying initial pH in O_3+CuO/ZnO system, the degradation efficiency of OFL increased with the increase of the initial pH value. By adjusting different levels of pH, it was found that although the final degradation rate changed little, the degradation rate of OFL changed significantly in the first 10 min. The results indicated that the degradation of OFL under alkaline condition was higher than that under acidic condition. When pH value was 11, the degradation efficiency of OFL after 30 min was 91%. The degradation efficiency of OFL could be improved under alkaline condition due to the fact that the presence of more OH^- enhanced the indirect oxidation and OH^- could combine with O_3 to generate more •OH [39].

3.8. Effect of initial OFL concentration

The initial pollutant concentration was also an important parameter in the O_3 catalytic process. Fig. 7d shows the degradation of OFL at various initial concentrations. When the initial OFL concentration increased from 10 to 50 mg/L, the degradation efficiency decreased from 89% to 59% after 30 min. The inhibitory effect of initial concentration on O_3 catalytic oxidation was consistent with that reported in the literature [52]. The reasons may be attributed to that excessive OFL and organic intermediates competitively consumed •OH [52].

3.9. Discussion on reaction mechanism of catalytic ozonation process

In order to confirm the enhancement of •OH generation in O_3+CuO/ZnO system, the formation of •OH in the non-catalytic ozonation system and the catalytic ozonation system was measured. 50 umol/L of benzoic acid was added to the non-catalytic ozonation system and the catalytic ozone system, and concentration of •OH was determined by measuring the concentration of p-HBA produced during the reaction of benzoic acid [53]. The results are shown in Fig. 8a. With the introduction of ozone into the solution, the formation of •OH increases rapidly in the non-catalytic ozonation and O_3+CuO/ZnO systems. However, the formation rate of •OH in the catalytic ozone system was much faster than that in the non-catalytic ozonation system, and the concentration of •OH was also higher than that in the non-catalytic ozonation process. These results suggested that CuO/ZnO could promote the generation •OH in the ozonation process.

It has been reported that tert-butanol (TBA) can be used to scavenge •OH and the reaction rate constant of TBA with hydroxyl radical was up to 6.0×10^8 M/s, and only 3.0×10^{-3} M/s with ozone [54]. In order to study whether existence of •OH in the O_3+CuO/ZnO catalytic ozonation system, quenching experiments were carried out using 5 mg/L TBA as radical scavengers. Fig. 8b illustrates that the presence of TBA significantly inhibited OFL degradation in both the ozonation alone and the catalytic ozonation system. Especially in

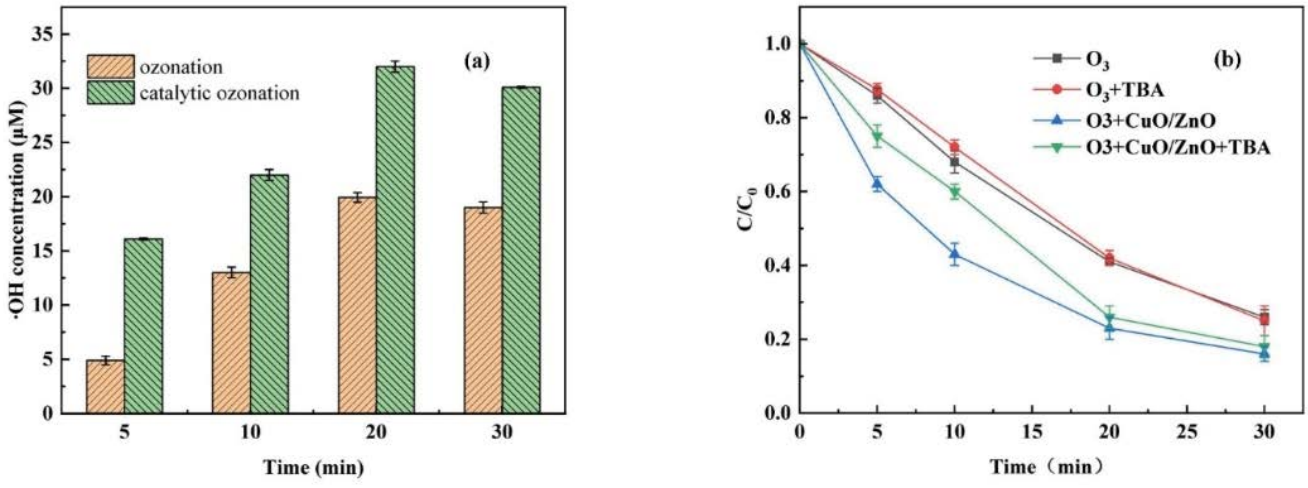

Fig. 8. (a) Formation of OH and (b) effect of TBA on the degradation of OFL.

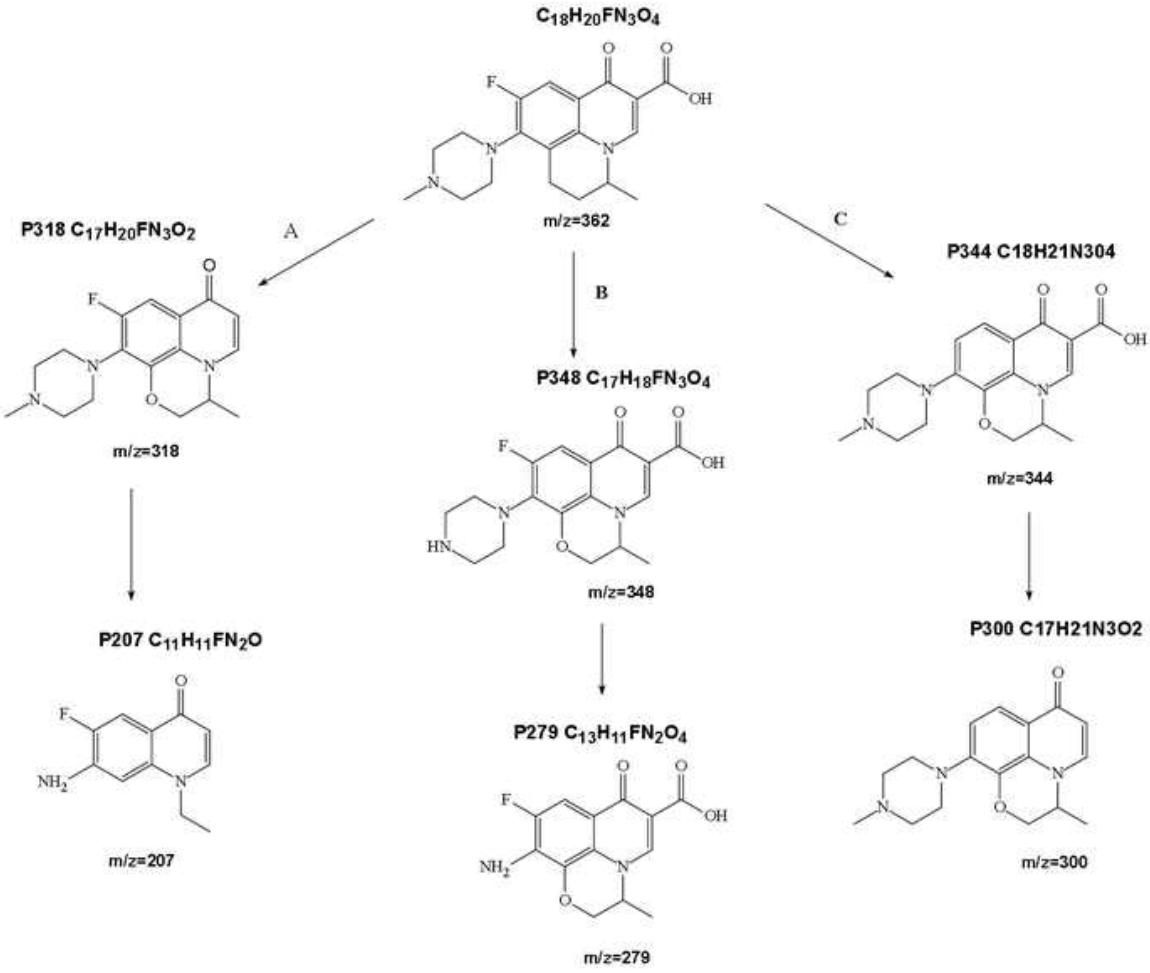

Fig. 9. OFL degradation products and possible degradation pathways. (Experimental conditions: $[OFL]_0$ = 20 mg/L, [ZnO] = [CuO] = [CuO/ZnO] = 0.63 g/L, $[O_3]$ = 80 mL/min, pH = 6.0).

the catalytic ozonation system, the degradation efficiency of OFL decreased from 57% to 40% within 10 min of oxidation time. This suggested that the quenching of •OH lead to the disappearance of the enhancement effect of catalytic ozonation on OFL degradation efficiency. It can be deduced that a large amount of •OH active species were produced in the catalytic ozonation system.

3.10. Degradation pathways of OFL

Catalytic ozonation produced a large number of complicate organic intermediates. The organic intermediates generated in the OFL degradation were analyzed by LC-MS/MS. As exhibited in Fig. 9, three possible degradation pathways (A, B and C) were proposed and outlined to identify these organic intermediates. The detailed mass spectral information for these compounds were given in Fig. S2 of the Supplementary materials. In pathway A, because the C–F bond of OFL was fragmented by the strong attack of·•OH, OFL was defluorinated and formed intermediate P344. Afterward, P344 was transformed to P300 by decarboxylation. In pathway B, OFL formed the intermediate product P348 by demethylation, the attack of •OH then leads to a

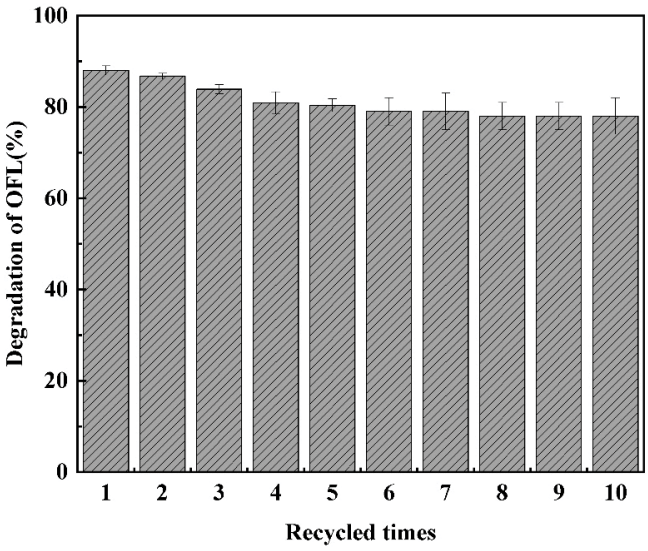

Fig. 10. Degradation of OFL with CuO/ZnO of different recycled times. Experimental conditions: $[OFL]_0$ = 20 mg/L, [CuO/ZnO] = 0.63 g/L, $[O_3]$ = 80 mL/min, pH = 6.0.

transformation of the piperazine ring on P348 to form the final product P279. In pathway C, the O_3+CuO/ZnO system decarboxylated OFL to produce the intermediate product P318. In the O_3+CuO/ZnO system, the cleavage of piperazine ring of P318 was to form the final product P207.

3.11. Stability of CuO/ZnO

Since the reusability of the catalyst is a key parameter, the stability of CuO/ZnO was also studied by the repeated OFL degradation experiments under the same conditions. As shown in Fig. 10, the catalytic ozonation system still has high OFL degradation efficiency after repeated use for 10 times. The slight changes proved that CuO/ZnO were stable and the reason could be due to the steady molecular structure. It was noteworthy that the maximum concentration of dissolved copper ion was determined less than 1.2 mg/L after 30 min. This was acceptable according to the EU discharge standards (<2 mg/L). The dissolution concentration of copper ions within 30 min of the reaction is shown in Fig. S3. These results indicated the high efficiency and stability of CuO/ZnO as O_3 catalyst that was beneficial to practical application.

4. Conclusion

CuO/ZnO with different CuO loading amounts was successfully synthesized by wet impregnation method and displayed highly catalytic activity toward ozonation in OFL degradation. Under the experimental conditions, the catalytic activity of CuO/ZnO catalyst was the highest when the CuO loading was 1:5. Under optimal conditions, the degradation of OFL by O_3+CuO/ZnO process was 88%, while that of O_3, O_3+ZnO and O_3+CuO were 74%, 76% and 78%, respectively. In addition, the operating parameters of catalytic ozonation have obvious influence on the degradation of OFL. The degradation rate of OFL was the highest when ozone flow was 80 mL/min, catalyst dose was 0.63 g/L, pH was 11 and OFL concentration was 10 mg/L. The presence of TBA limited the degradation of OFL in O_3+CuO/ZnO process, indicating that the presence of $^{\bullet}OH$ was the reason for the improvement of OFL degradation. The catalytic activity of CuO/ZnO decreased slightly after reused for 10 times, and the dissolution concentration of copper ions was less than 2 mg/L within 30 min. These results indicates that CuO/ZnO was a promising heterogeneous O_3 catalyst with high activity and stability.

Acknowledgements

This study was supported by the Natural Science Foundation of Guangxi Province (2020GXNSFAA159135), the Foundation (No.2021KF05) of Guangxi Key Laboratory of Clean Pulp & Papermaking and Pollution Control, College of Light Industry and Food Engineering, Guangxi University.

References

[1] B. Liu, Y. Li, Y. Wu, S. Xing, Enhanced degradation of ofloxacin by persulfate activation with Mn doped CuO: synergetic effect between adsorption and non-radical activation, Chem. Eng. J., 417 (2021) 127972, doi: 10.1016/j.cej.2020.127972.
[2] P. Sukul, M. Spiteller, Fluoroquinolone antibiotics in the environment, Rev. Environ. Contam. Toxicol., 191 (2007) 131–62.
[3] I. Ali, S. Afshinb, Y. Poureshgh, A. Azari, Y. Rashtbari, A. Feizizadeh, A. Hamzezadeh, M. Fazlzadeh, Green preparation of activated carbon from pomegranate peel coated with zero-valent iron nanoparticles (nZVI) and isotherm and kinetic studies of amoxicillin removal in water, Environ. Sci. Pollut. Res., 27 (2020) 36732–36743.
[4] D.G.J. Larsson, C. Pedro, N. Paxeus, Effluent from drug manufactures contains extremely high levels of pharmaceuticals, J. Hazard. Mater., 148 (2007) 751–755.
[5] C.L. Amorim, A.S. Maia, R.B.R. Mesquita, A.O.S.S. Rangel, M.C.M. Loosdrecht, M.E. Tiritan, P.M.L. Castro, Performance of aerobic granular sludge in a sequencing batch bioreactor exposed to ofloxacin, norfloxacin and ciprofloxacin, Water Res., 50 (2014) 101–103.
[6] S. Adhikari, H.H. Lee, D. Kim, Efficient visible-light induced electron-transfer in z-scheme MoO_3/Ag/C_3N_4 for excellent photocatalytic removal of antibiotics of both ofloxacin and tetracycline, Chem. Eng. J., 391 (2020) 123504, doi: 10.1016/j.cej.2019.123504.
[7] I. Michael, E. Hapeshi, C. Michael, D. Fatta-Kassinos, Solar Fenton and solar TiO_2 catalytic treatment of ofloxacin in secondary treated effluents: evaluation of operational and kinetic parameters, Water Res., 44 (2010) 5450–5462.
[8] Y. Zhang, R. Xiao, S. Wang, H. Zhu, H. Song, G. Chen, H. Lin, J. Zhang, J. Xiong, Oxygen vacancy enhancing Fenton-like catalytic oxidation of norfloxacin over prussian blue modified CeO_2: performance and mechanism, J. Hazard. Mater., 398 (2020) 122863, doi: 10.1016/j.jhazmat.2020.122863.
[9] X. Chen, M. Zhang, H. Qin, J. Zhou, Q. Shen, K. Wang, W. Chen, M. Liu, N. Li, Synergy effect between adsorption and heterogeneous photo-Fenton-like catalysis on $LaFeO_3$/lignin-biochar composites for high efficiency degradation of ofloxacin under visible light, Sep. Purif. Technol., 280 (2022) 119751, doi: 10.1016/j.seppur.2021.119751.
[10] Z. Berizi, S.Y. Hashemi, M. Hadi, A. Azari, A.H. Mahvi, The study of non-linear kinetics and adsorption isotherm models for Acid Red 18 from aqueous solutions by magnetite nanoparticles and magnetite nanoparticles modified by sodium alginate, Water Sci. Technol., 74 (2016) 1235–1242.
[11] S. Yousefzadeh, E. Ahmadi, M. Gholami, H.R. Ghaffari, A. Azari, M. Ansari, M. Miri, K. Sharafi, S. Rezaei, A comparative study of anaerobic fixed film baffled reactor and up-flow anaerobic fixed film fixed bed reactor for biological removal of diethyl phthalate from wastewater: a performance, kinetic, biogas, and metabolic pathway study, Biotechnol. Biofuels, 10 (2017), doi: 10.1186/s13068-017-0826-9.
[12] M. Moradi, A.M. Mansouri, N. Azizi, J. Amini, K. Karimi, K. Sharafi, Adsorptive removal of phenol from aqueous solutions by copper(Cu)-modified scoria powder: process modeling and kinetic evaluation, Desal. Water Treat., 57 (2016) 11820–11834.
[13] L. Yuan, J. Shen, Z. Chen, Y. Liu, Pumice-catalyzed ozonation degradation of p-chloronitrobenzene in aqueous solution, Appl. Catal., B, 117–118 (2021) 414–419.
[14] R. Amiri, A. Rezaei, N. Fattahi, M. Pirsaheb, J.R. Chueca, M. Moradi, Carbon quantum dots decorated Ag/$CuFe_2O_4$ for persulfate-assisted visible light photocatalytic degradation of tetracycline: a comparative study, J. Water Process Eng., 47 (2022) 102742, doi: 10.1016/j.jwpe.2022.102742.
[15] J. Wang, H. Chen, Catalytic ozonation for water and wastewater treatment: recent advances and perspective, Sci. Total Environ., 704 (2020) 135249, doi: 10.1016/j.scitotenv.2019.135249.
[16] Y.M. Dong, G.L. Wang, P.P. Jiang, A.M. Zhang, L. Yue, X.M. Zhang, Simple preparation and catalytic properties of ZnO for ozonation degradation of phenol in water, Chin. Chem. Lett., 22 (2011) 209–212.
[17] H. Jung, H. Choi, Catalytic decomposition of ozone and para-Chlorobenzoic acid (pCBA) in the presence of nanosized ZnO, Appl. Catal., B, 66 (2006) 288–294.
[18] M. Taie, A. Fadaei, M. Sadeghi, S. Hemati, G. Mardani, Comparison of the efficiency of ultraviolet/zinc oxide (UV/

ZnO) and ozone/zinc oxide (O_3/ZnO) techniques as advanced oxidation processes in the removal of trimethoprim from aqueous solutions, Int. J. Chem. Eng., 2021 (2021) 1–11.
[19] Z. Bai, Q. Yang, J. Wang, Catalytic ozonation of sulfamethazine using $Ce_{0.1}Fe_{0.9}OOH$ as catalyst: Mineralization and catalytic mechanisms, Chem. Eng. J., 300 (2016) 169–176.
[20] H. Zhao, Y. Dong, P. Jiang, G. Wang, J. Zhang, K. Li, An insight into the kinetics and interface sensitivity for catalytic ozonation: the case of nano-sized $NiFe_2O_4$, Catal. Sci. Technol., 4 (2014) 494–51.
[21] P. Xu, T. Wei, H. Yue, Y. Wen, Y. Wei, T. Guo, S. Li, W. Li, X. Wang, Effect of different nitric acid concentrations on manganese/activated carbon-modified catalysts for the catalytic ozonation of toluene, Catal. Sci. Technol., 10 (2020) 6729–6737.
[22] S. Kumar, A.K. Ojha, D. Bhorolua, J. Das, A. Kumar, A. Hazarika, Facile synthesis of CuO nanowires and Cu_2O nanospheres grown on rGO surface and exploiting its photocatalytic, antibacterial and supercapacitive properties, Physica B, 558 (2019) 74–81.
[23] M. Alavi, M. Moradi, Different antibacterial and photocatalyst functions for herbal and bacterial synthesized silver and copper/copper oxide nanoparticles/nanocomposites: a review, Inorg. Chem. Commun., 142 (2022) 109590, doi: 10.1016/j.inoche.2022.109590.
[24] O. Turkay, H. Inan, A. Dimoglo, Experimental and theoretical investigations of CuO-catalyzed ozonation of humic acid, Sep. Purif. Technol., 134 (2014) 110–116.
[25] J. Liu, J. Li, S. He, L. Sun, X. Yuan, D. Xia, Heterogeneous catalytic ozonation of oxalic acid with an effective catalyst based on copper oxide modified g-C_3N_4, Sep. Purif. Technol., 234 (2020) 116120, doi: 10.1016/j.seppur.2019.116120.
[26] A. Samad, M. Furukawa, H. Katsumata, T. Suzuki, S. Kaneco, Photocatalytic oxidation and simultaneous removal of arsenite with CuO/ZnO photocatalys, J. Photochem. Photobiol., A, 325 (2016) 97–103.
[27] C. Chen, X. Liu, Q. Fang, X. Chen, T. Liu, M. Zhang, Self-assembly and synthesis of CuOZnO hollow microspheres and their photocatalytic properties under natural light, Vacuum, 174 (2020) 109198, doi: 10.1016/j.vacuum.2020.109198.
[28] X. Zhang, X. He, Z. Kang, M. Cui, D.P. Yang, R. Luque, Waste eggshell-derived dual-functional CuO/ZnO/Eggshell nanocomposites: (photo)catalytic reduction and bacterial inactivation, ACS Sustainable Chem. Eng., 7 (2019) 15762–15771
[29] D. Kulawik, S. Zarska, A. Folentarska, V. Pavlyuk, W. Ciesielski, Synthesis, characterization, and catalytic properties of the Li-doped ZnO, J. Therm. Anal. Calorim., 134 (2018) 59–69.
[30] J. Vieillard, N. Bouazizi, M.N. Morshed, T. Clamens, F. Desriac, R. Bargougui, P. Thebault, O. Lesouhaitier, F.L. Derf, A. Azzouz, CuO nanosheets modified with amine and thiol grafting for high catalytic and antibacterial activities, Ind. Eng. Chem. Res., 58 (2019) 10179–10189.
[31] J. Peng, T. Lu, H. Ming, Z. Ding, Z. Yu, J. Zhang, Y. Hou, Enhanced photocatalytic ozonation of phenol by Ag/ZnO nanocomposites, Catalysts, 9 (2019) 1006, doi: 10.3390/catal9121006.
[32] T. Kamal, Aminophenols formation from nitrophenols using agar biopolymer hydrogel supported CuO nanoparticles catalyst, Polym. Test, 77 (2019) 105896, doi: 10.1016/j.polymertesting.2019.105896.
[33] W. Wang, H. Hu, X. Liu, H. Shi, T. Zhou, C. Wang, Z. Huo, Q. Wu, Combination of catalytic ozonation by regenerated granular activated carbon (rGAC) and biological activated carbon in the advanced treatment of textile wastewater for reclamation, Chemosphere, 231 (2019) 369–377.
[34] L. Xu, Y. Zhou, Z. Wu, G. Zheng, J. He, Y. Zhou, Improved photocatalytic activity of nanocrystalline ZnO by coupling with CuO, J. Phys. Chem. Solids, 106 (2017) 29–36.
[35] W. Sun, Y. Li, S. Ye, H. Rao, W. Yan, H. Peng, Y Li, Z. Liu, S. Wang, Z. Chen, L. Xiao, Z. Biao, C. Huang High-performance inverted planar heterojunction perovskite solar cells based on solution-processed CuO_X hole transport layer, Nanoscale, 8 (2016) 10806–10813
[36] W. Wang, L. Xu, R. Zhang, J. Xu, F. Xian, J. Su, F. Yang, Coexistence of ferromagnetism and paramagnetism in ZnO/CuO nanocomposites, Chem. Phys. Lett., 721 (2019) 57–61.
[37] Y. Huang, Y. Sun, Z. Xu, M. Luo, C. Zhu, L. Li, Removal of aqueous oxalic acid by heterogeneous catalytic ozonation with MnOx/sewage sludge-derived activated carbon as catalysts, Sci. Total Environ., 575 (2017) 50–57.
[38] Y. Bao, K. Chen, A novel Z-scheme visible light driven Cu_2O/Cu/g-C_3N_4 photocatalyst using metallic copper as a charge transfer mediator, Mol. Catal., 432 (2017) 187–195.
[39] X. Lu, S. Xie, S. Li, J. Zhou, W. Sun, Y. Xu, Y. Sun, Treatment of purified terephthalic acid wastewater by ozone catalytic oxidation method, Water, 13 (2021) 1906.
[40] G. Scaratti, A. Basso, R. Landers, P.J.J. Alvarez, G.L. Puma, R.F.P.M. Moreira, Treatment of aqueous solutions of 1,4-dioxane by ozonation and catalytic ozonation with copper oxide (CuO), Environ. Technol., 41 (2020) 1464–1476.
[41] R. Huang, H. Yan, L. Li, D. Deng, Y. Shu, Q. Zhang, Catalytic activity of Fe/SBA-15 for ozonation of dimethyl phthalate in aqueous solution, Appl. Catal., B, 106 (2011) 264–271.
[42] A. Abdedayem, M. Guiza, F.J.R. Toledo, A. Ouederni, Nitrobenzene degradation in aqueous solution using ozone/cobalt supported activated carbon coupling process: a kinetic approach, Sep. Purif. Technol., 184 (2017) 308–318.
[43] S. Tang, D. Yuan, Q. Zhang, Y. Liu, Q. Zhang, Z. Liu, H. Huang, Fe-Mn bi-metallic oxides loaded on granular activated carbon to enhance dye removal by catalytic ozonation, Environ. Sci. Pollut. Res., 23 (2016) 18800–18808.
[44] L. Li, W. Ye, Q. Zhang, F. Sun, P. Lu, X. Li, Catalytic ozonation of dimethyl phthalate over cerium supported on activated carbon, J. Hazard. Mater., 170 (2009) 411–416.
[45] Y. Vasseghian, F. Almomani, V.T. Le, M. Moradi, E. Dragoi, Decontamination of toxic Malathion pesticide in aqueous solutions by Fenton-based processes: degradation pathway, toxicity assessment and health risk assessment, J. Hazard. Mater., 423 (2022) 127016, doi: 10.1016/j.jhazmat.2021.127016.
[46] Z.Y. Bai, Q. Yang, J.L. Wang, Fe_3O_4/multi-walled carbon nanotubes as an efficient catalyst for catalytic ozonation of p-hydroxybenzoic acid, Int. J. Environ. Sci. Technol., 13 (2016) 483–492.
[47] Q. Dai, J. Wang, J. Yu, J. Chen, J. Chen, Catalytic ozonation for the degradation of acetylsalicylic acid in aqueous solution by magnetic CeO_2 nanometer catalyst particles, Appl. Catal., B, 144 (2014) 686–693.
[48] Y. Huaccallo, S. Álvarez-Torrellas, M.P. Marin, M.V. Gil, M. Larriba, V.I. Águeda, G. Ovejero, J. Garcia, Magnetic Fe_3O_4/multi-walled carbon nanotubes materials for a highly efficient depletion of diclofenac by catalytic wet peroxide oxidation, Environ. Sci. Pollut. Res., 26 (2019) 22372–22388.
[49] J. Wang, Z. Bai, Fe-based catalysts for heterogeneous catalytic ozonation of emerging contaminants in water and wastewater, Chem. Eng. J., 312 (2017) 79–98
[50] B. Kasprzyk-Hordern, M. Ziółek, J. Nawrocki, Catalytic ozonation and methods of enhancing molecular ozone reactions in water treatment, Appl. Catal. B, 46 (2003) 639–669.
[51] R. Huang, B. Lan, Z. Chen, H. Yan, Q. Zhang, J. Bing, L. Li, Catalytic ozonation of p-chlorobenzoic acid over MCM-41 and Fe loaded MCM-41, Chem. Eng. J., 180 (2012) 19–24.
[52] J. Akhtar, N.S. Amin, A. Aris, Combined adsorption and catalytic ozonation for removal of sulfamethoxazole using Fe_2O_3/CeO_2 loaded activated carbon, Chem. Eng. J., 170 (2011) 136–144.
[53] L. Chen, J. Ma, X. Li, J. Zhang, J. Fang, Y. Guan, P. Xie, Strong enhancement on fenton oxidation by addition of hydroxylamine to accelerate the ferric and ferrous iron cycles, Environ. Sci. Technol., 45 (2011) 3925–3930.
[54] L. Xu, J. Wang, Magnetic nanoscaled Fe_3O_4/CeO_2 composite as an efficient Fenton-like heterogeneous catalyst for degradation of 4-chlorophenol, Environ. Sci. Technol., 46 (2012) 10145–10153.

Supplementary information

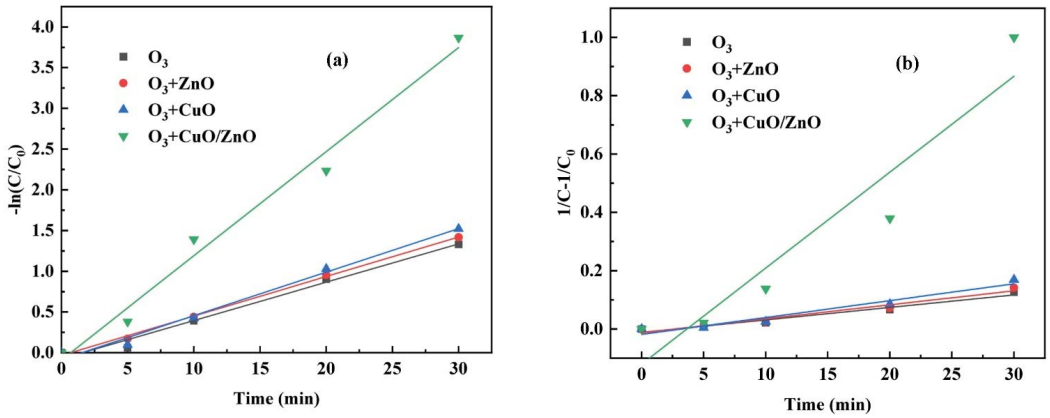

Fig. S1. (a) Pseudo-first-order kinetic fitting of OFL removal and (b) pseudo-second-order kinetic fitting of OFL removal.

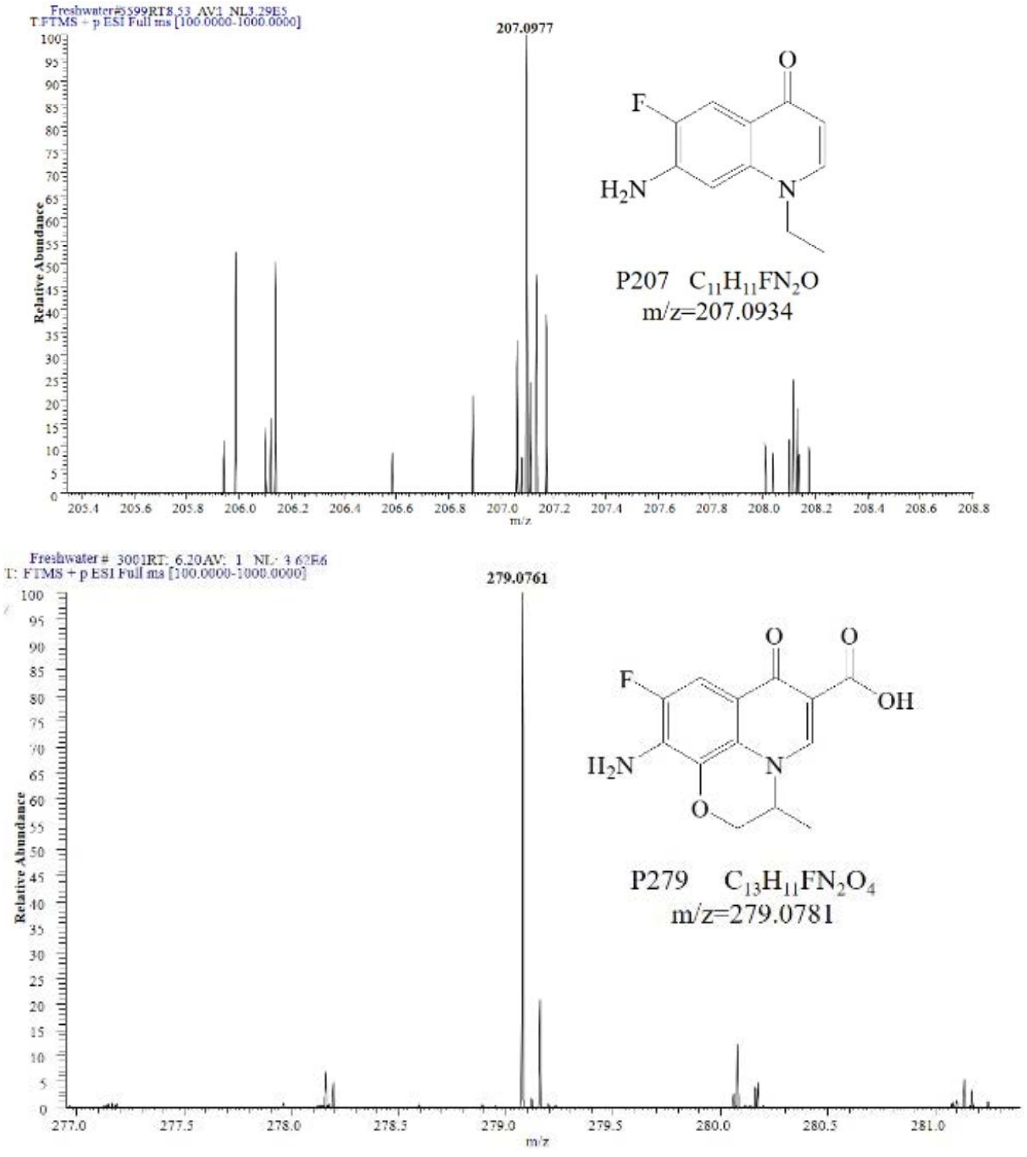

Fig. S2. (Continued)

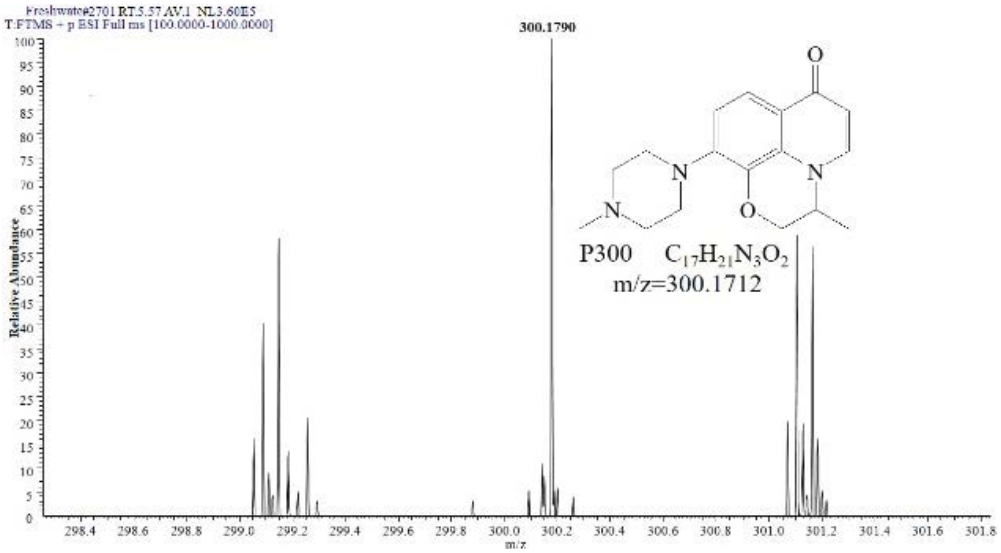

Fig. S2. Final mass spectrum after OFL reaction.

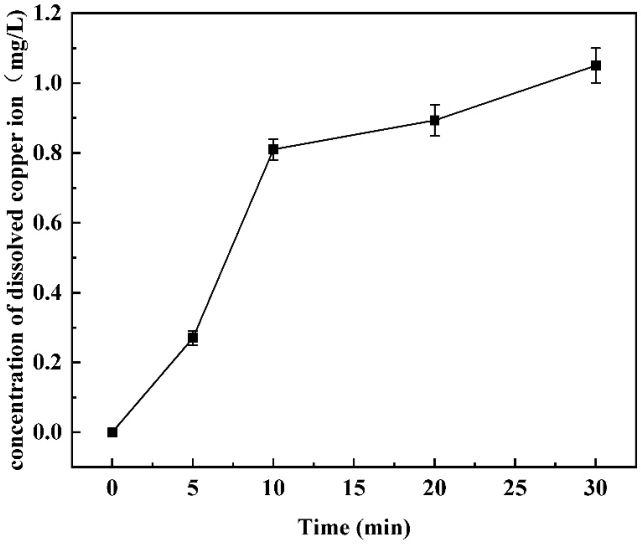

Fig. S3. Concentration of dissolved copper ions for 30 min of reaction.

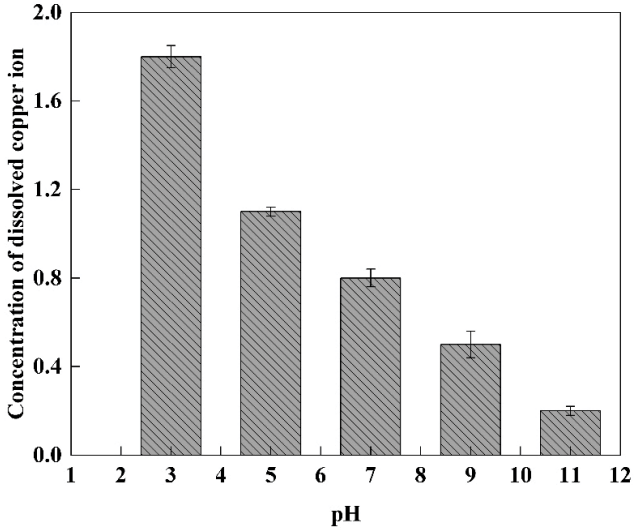

Fig. S4. Concentration of dissolved copper ion with different pH.

Table S1
Comparison with recent articles

Articles	Comparison of results
Catalytic activity of Fe/SBA-15 for ozonation of dimethyl phthalate in aqueous solution	Ozone flow rate: 800 mL/min, Ozone flow rate used in this paper: 80 mL/min
Treatment of purified terephthalic acid wastewater by ozone catalytic oxidation method	The removal rate of pollutants in 50 min was 74.28%, in this paper: the removal rate of pollutants in 30 min was 88%.
Nitrobenzene degradation in aqueous solution using ozone/cobalt supported activated carbon coupling process: a kinetic approach	The dose of catalyst used was 1 g/L, in this paper: the dose of catalyst used was 0.63 g/L
Treatment of aqueous solutions of 1,4-dioxane by ozonation and catalytic ozonation with copper oxide (CuO)	The removal rate of pollutants was 78%, in this paper: the removal rate of pollutants was 88%.
Fe-Mn bi-metallic oxides loaded on granular activated carbon to enhance dye removal by catalytic ozonation.	The dose of catalyst used was 2.5 g/L, in this paper: the dose of catalyst used was 0.63 g/L. Ozone flow rate: 2 L/min, Ozone flow rate used in this paper: 80 mL/min.

Table S2
Comparison of first-order and second-order kinetics fitting for OFL removal among different processes.

Process	First-order		Second-order	
	k_1 (min^{-1})	R^2	k_2 ($L \cdot mg^{-1} \cdot min^{-1}$)	R^2
O_3	0.047	0.98246	0.00429	0.95493
O_3+ZnO	0.04844	0.99693	0.00479	0.95156
O_3+CuO	0.05346	0.98978	0.00579	0.94035
O_3+CuO/ZnO	0.12784	0.97956	0.03288	0.87834